



Revised upper limits for abundances of NH₃, HCN and HC₃N in the Martian atmosphere

A. Trokhimovskiy, A.A. Fedorova, Franck Lefèvre, O. Korablev, Kevin S. Olsen, J. Alday, D. Belyaev, Franck Montmessin, A. Patrakeev, N. Kokonkov

► To cite this version:

A. Trokhimovskiy, A.A. Fedorova, Franck Lefèvre, O. Korablev, Kevin S. Olsen, et al.. Revised upper limits for abundances of NH₃, HCN and HC₃N in the Martian atmosphere. *Icarus*, 2024, 407 (January), pp.115789. 10.1016/j.icarus.2023.115789 . insu-04211677

HAL Id: insu-04211677

<https://insu.hal.science/insu-04211677v1>

Submitted on 12 Jan 2025

HAL is a multi-disciplinary open access archive for the deposit and dissemination of scientific research documents, whether they are published or not. The documents may come from teaching and research institutions in France or abroad, or from public or private research centers.

L'archive ouverte pluridisciplinaire **HAL**, est destinée au dépôt et à la diffusion de documents scientifiques de niveau recherche, publiés ou non, émanant des établissements d'enseignement et de recherche français ou étrangers, des laboratoires publics ou privés.



Distributed under a Creative Commons Attribution 4.0 International License

1 Revised upper limits for abundances of NH₃, HCN and HC₃N in
2 the Martian atmosphere

3
4 A. Trokhimovskiy¹, A. A. Fedorova¹, F. Lefèvre², O. Koralev¹, K.S. Olsen³, J. Alday⁴,
5 D. Belyaev¹, F. Montmessin², A. Patrakeev¹, N. Kokonkov¹

6
7 ¹ Space Research Institute (IKI) RAS, Moscow, Russia

8 e-mail: trokh@cosmos.ru

9 ² LATMOS/CNRS, Guyancourt, France

10 ³ Department of Physics, University of Oxford, Oxford, UK

11 ⁴ The Open University, Milton Keynes, UK

12
13 **Abstract**

14 The Atmospheric Chemistry Suite (ACS) onboard the ExoMars Trace Gas Orbiter (TGO)
15 spacecraft has been studying Mars' atmosphere since 2018. The sensitivity of the middle
16 infrared channel (MIR) allows it to address many ardent topics and it is capable of improving
17 and establishing upper limits for many trace species. In this work we present analysis of
18 transmittance spectra in the 3332.5–3338.6 cm⁻¹ range with 30,000 resolution ($\lambda/\Delta\lambda$),
19 covering absorptions lines of three nitrogen-bearing species: ammonia (NH₃), hydrogen cyanide
20 (HCN) and cyanoacetylene (HC₃N). According to existing models, all of those are not expected
21 to be present in a CO₂-rich Martian atmosphere, but outgassing or unknown chemistry sources
22 cannot be discounted. The upper limits of 14, 1.5 and 11 ppbv are obtained for NH₃, HCN and
23 HC₃N from individual occultation measurements during the warm and dusty perihelion season
24 of martian year 36. For the ammonia and hydrogen cyanide the upper limits are improved
25 compared to previously published results. A search for cyanoacetylene on Mars is reported for
26 the first time.

27
28 **Keywords:** IR spectroscopy; Mars, atmosphere; Atmospheres, composition

29
30 **Main**

31 Molecular nitrogen is the second most abundant species (2.8%) after CO₂ in the Martian
32 atmosphere (Franz et al., 2017). Soil contains oxidised nitrogen-bearing compounds (Stern et
33 al., 2015; Sutter et al., 2017). Also the chemically-derivatized molecules ammonia (NH₃) and
34 hydrogen cyanide (HCN) were detected from sand, among others, with the wet chemistry
35 experiments of the Sample Analysis at Mars (SAM) instrument on NASA's Curiosity rover
36 (Millan et al., 2022). The combination of an elevated abundance of derivatized ammonia and
37 several N-bearing organic species detected in the follow-up analyses suggested that
38 indigenous N-bearing molecules are present in the soil. At the same time, expected
39 atmospheric processes involving nitrogen are limited (Lefèvre and Krasnopolsky, 2017),
40 because the strong N–N bond makes N₂ a relatively inert species. Odd-nitrogen species, N and
41 NO, can be produced as a result of N₂ dissociation at high altitudes only. The nitrogen
42 chemistry in the lower atmosphere thus greatly depends on the downward fluxes. As calculated
43 by the general circulation model of Moudden and McConnell (2007), main nitrogen species
44 below 40 kilometres are NO and NO₂, varying in tiny abundances from 0.1 ppbv to 0.25 ppbv.
45 The current knowledge for NO₂ is <10 ppbv (Maguire, 1977) and less than 1.7 ppb for NO
46 (Krasnopolsky, 2006). The sensitivity of the mid-infrared channel of the Atmospheric Chemistry
47 Suite (ACS MIR) approaches the expected NO₂ 0.2 ppbv absorption features in the 2915 cm⁻¹

48band, which will be a subject of a separate study. Not considering any release processes, other
49nitrogen components are modelled to be orders of magnitude less abundant, like the pptv level
50concentrations of HNO_4 near 20 km in altitude.

51 In this work we present upper limits of somewhat unexpected molecules for Mars:
52ammonia, hydrogen cyanide and cyanoacetylene derived from ACS MIR data. The first two
53have been already searched for on Mars, the third has not yet been considered.

54 As in the case of methane (CH_4), the ammonia could be considered as a biomarker. But
55in contrast to methane, whose lifetime is considered to be on the order of a hundred years
56(Lefèvre and Krasnopolksy, 2017), ammonia is not a stable molecule in the atmosphere of Mars
57and would be quickly photolyzed within hours. Hydrogen cyanide is also not expected to be
58produced in the Martian atmosphere (Mancinelli and Banin, 2003): its permanent presence
59would require a continuous source, like active volcanoes or biota, both actively sought, but
60never detected on Mars.

61 The first NH_3 3 ? upper limit of 8 ppbv was set by the Mariner 9 Infrared Interferometer
62Spectrometer (IRIS; Maguire, 1977). The results were obtained from an average of spectra
63from all over the planet, covering a full Martian year (MY), starting from $L_s = 293^\circ$ in MY 9. In
642004, the detection of ammonia in the atmosphere of Mars by the Planetary Fourier
65Spectrometer (PFS) was announced; the report was not followed by a publication. The NH_3
66was then sought using NIRSPEC at Keck-2 observatory (Villanueva et al., 2013). The
67observations at $L_s = 352^\circ$ in MY 27 provided a 57 ppbv 3 ? upper limit, and at $L_s = 83^\circ$ in MY
6830, a 45 ppbv upper limit. In parallel, they have established HCN upper limits of 4.5 and 2.1
69ppbv, respectively.

70 HC_3N was not considered as a goal for Martian atmospheric surveys, while it has a
71notable astrochemical importance (e.g. Thelen et al., 2019; Jiang et al., 2017). The most recent
72version of the spectroscopy database HITRAN2020 (Gordon et al., 2022) includes, for the first
73time, ro-vibrational transitions relative to all seven vibrational modes of HC_3N up to 3400 cm^{-1} .
74and rotational data in the ground state and many vibrational states of all normal modes. In this
75work, we used the recently documented band around 3327 cm^{-1} to set the first upper limit on
76 HC_3N in Mars atmosphere.

77 The ACS package for the Trace Gas Orbiter (TGO) is a part of the ExoMars mission
78(Korablev et al., 2018; Vago et al., 2015). ACS includes the mid-infrared channel (MIR), a
79versatile instrument for the spectral range 2.3-4.2 μm . It is a cross-dispersion echelle
80instrument dedicated to solar occultation measurements. The resolving power of 30,000 and a
81signal-to-noise ratio (SNR) of 5,000 per pixel per 2 s acquisition make it perfect for detecting
82weak absorptions (Trokhimovskiy et al., 2020; Olsen et al., 2020). We use the ACS MIR
83measurements obtained using secondary grating position 13, which includes 27 diffraction
84orders (190-216) encompassing a spectral range of $3178\text{-}3643 \text{ cm}^{-1}$. Order 199 covers a range
85 $3330.5\text{-}3355.1 \text{ cm}^{-1}$, where all three gases, NH_3 , HCN, and HC_3N , have absorption lines . This
86range also contains CO_2 and H_2O lines, which are used for additional pixel-to-wavenumber
87calibration. To retrieve upper limits in this work, we used a narrower $3332.5\text{-}3338.6 \text{ cm}^{-1}$ fitting
88window (see Figure 1 Panel A for model spectra of sought gases and data example).

89 Regular and optimised position 13 measurements have started mid MY 36. The dataset
90analysed includes 135 ACS MIR occultations performed in MY 36 during southern summer at
91the perihelion season ($L_s = 212^\circ\text{-}360^\circ$; TGO orbits 19,656-22,705). The observation period is
92characterised by greater dust load, higher temperatures, elevation of water vapour up to
93120 km (Belyaev et al., 2021; Fedorova et al., 2023). Recently discovered by ACS, hydrogen
94chloride is being observed exceptionally in the perihelion season (Korablev et al., 2021; Olsen
95et al., 2021), emphasising more active atmospheric chemistry. The observed latitudes range

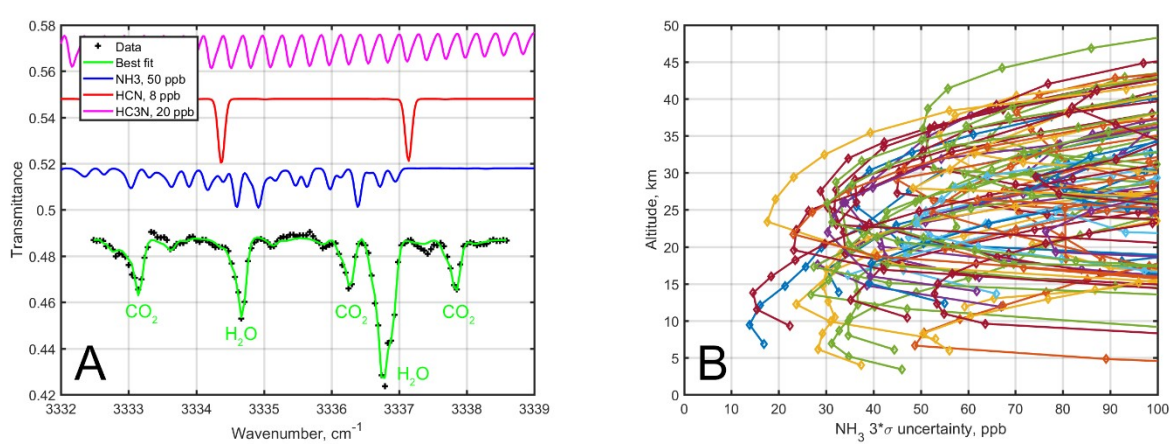
96from -77°S to 90°N , with the majority of occultations occurring at high latitudes (Korablev et al., 972018).

98 The retrieval is performed by the iterative Levenberg–Marquardt iterative algorithm with
99 Tikhonov regularisation developed to analyse data from SPICAM IR spectrometer on Mars
100 Express (Fedorova et al., 2018) and TGO’s ACS near-infrared channel (NIR) data (Fedorova et
101 al., 2020) and adapted for ACS MIR data (Trokhimovskiy et al., 2021; Fedorova et al., 2022).
102 The CO_2 density and temperature profiles were not retrieved, but taken from ACS NIR
103 simultaneous measurements (Korablev et al., 2018; Fedorova et al., 2023). The free
104 parameters are aerosol extinction and volume mixing ratios of gases. In the absence of
105 detection, the uncertainty on the retrieved quantities is given by the covariance matrix of the
106 solution, which defines the upper limit. The retrieved values are generally within a 1? away
107 from zero; we present the three-sigma upper limits as a confident non-detection case. The
108 vertical dependence of the upper limits is typical for occultation experiments and for Mars
109 reaches the best values at altitudes of about 10–25 km. At higher altitudes, the line-of-sight
110 captures only a miserable number of searched molecules, at lower altitudes the signal is
111 diminished by aerosol load. On Figure 1 Panel B we present a collection of three-sigma upper
112 limits for NH_3 from different orbits. The vertical pattern for HCN and HC_3N is similar.

113 The best upper limits are achieved at $L_s = 233^{\circ}$, latitude 64°N and altitude 10 km, and
114 accordingly for NH_3 , HCN and HC_3N are 14, 1.5 and 11 ppbv. Tens of observations provide
115 upper limits below 33, 3.5 and 30 ppbv at high latitudes in both hemispheres during the whole
116 season observed. The upper limit for HC_3N is not restrictive since HCN is typically the most
117 abundant nitrile. At lower latitudes, with more aerosols and less occultations available, the best
118 upper limits by ACS MIR for NH_3 , HCN and HC_3N were 114, 12 and 95 ppbv. These numbers
119 were achieved at $L_s = 287^{\circ}$, latitude -12°S and altitude 39 km.

120 The upper limits for ammonia and hydrogen cyanide are several times below those
121 obtained by Villanueva et al. (2013) for the end of MY 27. Moreover, the ACS data cover the
122 entire perihelion season and different latitudes. The upper limits for cyanoacetylene in the
123 Martian atmosphere are obtained for the first time. Tracing these species, unexpected on Mars,
124 with stringent upper limits is important to monitor potential outgassing events and constrain
125 chemical models. As the ExoMars mission continues, ACS will extend the trace species search
126 further.

127



128
129

130 Figure 1. Panel A. Example of ACS MIR data from order 199 and the best fit at tangent
131 altitude 18 km, orbit 21352 N1, $L_s = 299^{\circ}$, latitude -55°S . The model spectra for NH_3 , HCN and
132 HC_3N are shown shifted and with abundances of 50, 8 and 20 ppbv, respectively. The

133noticeable lines fitted in the data are due to CO₂ and are located at 3333.1, 3336.2 and 3337.8
134cm⁻¹, the H₂O line is at 3334.6 cm⁻¹ and a doublet around 3336.8 cm⁻¹. Panel B. The vertical
135dependency of the three-sigma upper limits for ammonia from the ACS MIR solar occultation
136observations. The vertical pattern for HCN and HC₃N is similar. Different colours stand for
137distinct occultations.

138

139

140Belyaev, D., Fedorova, A.A., Trokhimovskiy, A., Alday, J., Montmessin, F., Koralev, O.I.,
141 Lefèvre, F., Patrakeev, A.S., Olsen, K.S., Shakun, A.V., 2021. Revealing a high water
142 abundance in the upper mesosphere of Mars with ACS onboard TGO. *J. Geophys. Res.*
143 Letters, Volume48, Issue10. <https://doi.org/10.1029/2021GL093411>

144Franz, H.B. et al. 2017. Initial SAM calibration gas experiments on Mars: Quadrupole mass
145 spectrometer results and implications. *Planetary and Space Science* 138, 44–54.
146 doi:10.1016/j.pss.2017.01.014

147Fedorova, A., Bertaix, J.-L., Betsis, D., Montmessin, F., Koralev, O., Maltagliati, L., Clarke,
148 J., 2018. Water vapor in the middle atmosphere of Mars during the 2007 global dust
149 storm. *Icarus*. 300, pp. 440-457. <https://doi.org/10.1016/j.icarus.2017.09.025>.

150Fedorova, A.A., Montmessin, F., Koralev, O., Luginin, M., Trokhimovskiy, A., Belyaev, D.A.,
151 Ignatiev, N.I., Lefèvre, F., Alday, J., Irwin, P.G.J., Olsen, K.S., Bertaix, J.-L., Millour, E.,
152 Määttänen, A., Shakun, A., Grigoriev, A.V., Patrakeev, A., Korsa, S., Kokonkov, N.,
153 Baggio, L., Forget, F., Wilson, C.F., 2020. Stormy water on Mars: The distribution and
154 saturation of atmospheric water during the dusty season. *Science*. 367, pp. 297-300.
155 <https://doi.org/10.1126/science.aay9522>.

156Fedorova, A., Trokhimovskiy, A., Lefèvre, F., Olsen, K.S., Koralev, O., Montmessin, F.,
157 Ignatiev, N., Lomakin, A., Forget, F., Belyaev, D., Alday, J., Luginin, M., Smith, M.,
158 Patrakeev, A., Shakun, A., Grigoriev, A., 2022. Climatology of the CO vertical distribution
159 on Mars based on ACS TGO measurements. *J. Geophys. Res.: Planets*. 127,
160 e2022JE007195. <https://doi.org/10.1029/2022JE007195>.

161Fedorova, A.A., Montmessin, F., Trokhimovskiy, A., Luginin, M., Koralev, O., Alday, J.,
162 Belyaev, D., Holmes, J., Lefevre, F., Olsen, K., Patrakeev, A., Shakun, F. 2023. A two-
163 martian years survey of the water vapor saturation state on Mars based on ACS
164 NIR/TGO occultations. *J. Geophys. Res.: Planets*. e2022JE007348.
165 <https://doi.org/10.1029/2022JE007348>

166Gordon, I.E., Rothman, L.S., Hargreaves, R.J., Hashemi, R., Karlovets, E.V., Skinner, F.M.,
167 Conway, E.K., Hill, C., Kochanov, R.V., Tan, Y., Wcisło, P., Finenko, A.A., Nelson, K.,
168 Bernath, P.F., Birk, M., Boudon, V., Campargue, A., Chance, K.V., Coustenis, A., Drouin,
169 B.J., Flaud, J.-M., Gamache, R.R., Hodges, J.T., Jacquemart, D., Mlawer, E.J., Nikitin,
170 A.V., Perevalov, V.I., Rotger, M., Tennyson, J., Toon, G.C., Tran, H., Tyuterev, V.G.,
171 Adkins, E.M., Baker, A., Barbe, A., Canè, E., Császár, A.G., Dudaryonok, A., Egorov, O.,
172 Fleisher, A.J., Fleurbaey, H., Foltynowicz, A., Furtenbacher, T., Harrison, J.J., Hartmann,
173 J.-M., Horneman, V.-M., Huang, X., Karman, T., Karns, J., Kassi, S., Kleiner, I., Kofman,
174 V., Kwabia-Tchana, F., Lavrentieva, N.N., Lee, T.J., Long, D.A., Lukashevskaya, A.A.,
175 Lyulin, O.M., Makhnev, V.Yu., Matt, W., Massie, S.T., Melosso, M., Mikhailenko, S.N.,
176 Mondelain, D., Müller, H.S.P., Naumenko, O.V., Perrin, A., Polyansky, O.L., Raddaoui, E.,
177 Raston, P.L., Reed, Z.D., Rey, M., Richard, C., Tóbiás, R., Sadiek, I., Schwenke, D.W.,
178 Starikova, E., Sung, K., Tamassia, F., Tashkun, S.A., Vander Auwera, J., Vasilenko, I.A.,
179 Vigasin, A.A., Villanueva, G.L., Vispoe, B., Wagner, G., Yachmenev, A., Yurchenko,

- 180 S.N., 2022. The HITRAN2020 molecular spectroscopic database. J.Q.S.R.T. 277,
181 107949. <https://doi.org/10.1016/j.jqsrt.2021.107949>.
- 182 Jiang, X.-J., Wang, J.-Z., Gao Y., Gu, Q.-S., 2017. HC3N observations of nearby galaxies.
183 A&A. 600, A15. <https://doi.org/10.1051/0004-6361/201629066>.
- 184 Koralev, O., Montmessin, F., Trokhimovskiy, A., Fedorova, A.A., Shakun, A.V., Grigoriev,
185 A.V., Moshkin, B.E., Ignatiev, N.I., Forget, F., Lefèvre, F., Anufreychik, K., Dzuban, I.,
186 Ivanov, Y.S., Kalinnikov, Y.K., Kozlova, T.O., Kungurov, A., Makarov, V., Martynovich, F.,
187 Maslov, I., Merzlyakov, D., Moiseev, P.P., Nikolskiy, Y., Patrakeev, A., Patsaev, D.,
188 Santos-Skipko, A., Sazonov, O., Semena, N., Semenov, A., Shashkin, V., Sidorov, A.,
189 Stepanov, A. V., Stupin, I., Timonin, D., Titov, A.Y., Viktorov, A., Zharkov, A., Altieri, F.,
190 Arnold, G., Belyaev, D.A., Bertaux, J. L., Betsis, D.S., Duxbury, N., Encrenaz, T.,
191 Fouchet, T., Gérard, J.-C., Grassi, D., Guerlet, S., Hartogh, P., Kasaba, Y., Khatuntsev,
192 I., Krasnopolsky, V.A., Kuzmin, R.O., Lellouch, E., Lopez-Valverde, M.A., Luginin, M.,
193 Määttänen, A., Marcq, E., Martin Torres, J., Medvedev, A.S., Millour, E., Olsen, K.S.,
194 Patel, M.R., Quantin-Nataf, C., Rodin, A.V., Shematovich, V.I., Berkenbosch, I.,
195 Thomas, N., Vazquez, L., Vincendon, M., Wilquet, V., Wilson, C.F., Zasova, L.V., Zelenyi,
196 L.M., Zorzano, M.P., 2018. The Atmospheric Chemistry Suite (ACS) of Three
197 Spectrometers for the ExoMars 2016 Trace Gas Orbiter. Space Sci. Rev. 214, 7.
198 <https://doi.org/10.1007/s11214-017-0437-6>.
- 199 Koralev, O., Olsen, K.S., Trokhimovskiy, A., Lefèvre, F., Montmessin, F., Fedorova, A.A.,
200 Toplis, M.J., Alday, J., Belyaev, D.A., Patrakeev, A., Ignatiev, N.I., Shakun, A.V.,
201 Grigoriev, A.V., Baggio, L., Abdenour, I., Lacombe, G., Ivanov, Y.S., Aoki, S., Thomas,
202 I.R., Daerden, F., Ristic, B., Erwin, J.T., Patel, M., Bellucci, G., Lopez-Moreno, J.-J.,
203 Vandaele, A.C., 2021. Transient HCl in the atmosphere of Mars. Sci. Adv. 7, eabe4386.
204 <https://doi.org/10.1126/sciadv.abe4386>.
- 205 Krasnopolsky, V.A. 2006. A sensitive search for nitric oxide in the lower atmospheres of Venus
206 and Mars: Detection on Venus and upper limit for Mars. Icarus 182, 80–91.
207 doi:10.1016/j.icarus.2005.12.003
- 208 Lefèvre, F., Krasnopolsky, V., 2017. Atmospheric Photochemistry. In: Haberle, R.M., Clancy,
209 R.T., Forget, F., Smith, M.D., Zurek, R.W. (Eds.), The Atmosphere and Climate of Mars,
210 pp. 405 - 432. <http://dx.doi.org/10.1017/9781139060172.013>.
- 211 Maguire, W.C., 1977. Martian isotopic ratios and upper limits for possible minor constituents as
212 derived from Mariner 9 infrared spectrometer data. Icarus. 32, pp. 85–97.
213 [https://doi.org/10.1016/0019-1035\(77\)90051-3](https://doi.org/10.1016/0019-1035(77)90051-3).
- 214 Mancinelli, R.L., Banin, A., 2003. Where is the nitrogen on Mars? Int. J. Astrobiol. 2, pp. 217–
215 225. <https://doi.org/10.1017/S1473550403001599>.
- 216 Millan, M., Teinturier, S., Malespin, C.A., Bonnet, J.Y., Buch, A., Dworkin, J.P., Eigenbrode,
217 J.L., Freissinet, C., Glavin, D.P., Navarro-González, R., Srivastava, A., Stern, J.C., Sutter,
218 B., Szopa, C., Williams, A.J., Williams, R.H., Wong, G.M., Johnson, S.S., Mahaffy, P. R.,
219 2022. Organic molecules revealed in Mars's Bagnold Dunes by Curiosity's derivatization
220 experiment. Nat. Astron. 6, pp. 129–140. <https://doi.org/10.1038/s41550-021-01507-9>.
- 221 Montmessin, F., Koralev, O.I., Trokhimovskiy, A., Lefèvre, F., Fedorova, A.A., Baggio, L.,
222 Irbah, A., Lacombe, G., Olsen, K.S., Braude, A.S., Belyaev, D.A., Alday, J., Forget, F.,
223 Daerden, F., Pla-Garcia, J., Rafkin, S., Wilson, C.F., Patrakeev, A., Shakun, A., Bertaux,
224 J.L., 2021. A stringent upper limit of 20 pptv for methane on Mars and constraints on its
225 dispersion outside Gale crater. A&A. 650, A140. <https://doi.org/10.1051/0004-6361/202140389>.

- 227 Moudden Y., McConnell, J.C., 2007. Three-dimensional on-line chemical modelling in a Mars
228 general circulation model. *Icarus*. 188, pp. 18-34.
229 <http://dx.doi.org/10.1016/j.icarus.2006.11.005>.
- 230 Olsen, K.S., Lefèvre, F., Montmessin, F., Trokhimovskiy, A., Baggio, L., Fedorova, A.A., Alday,
231 J., Lomakin, A., Belyaev, D.A., Patrakeev, A., Shakun, A., Koralev, O.I., 2020. First
232 detection of ozone in the mid-infrared at Mars: implications for methane detection. *A&A*.
233 639, A141. <https://doi.org/10.1051/0004-6361/202038125>.
- 234 Olsen, K.S., Trokhimovskiy, A., Montabone, L., Fedorova, A.A., Luginin, M., Lefèvre, F.,
235 Koralev, O.I., Montmessin, F., Forget, F., Millour, E., Bierjon, A., Baggio, L., Alday, J.,
236 Wilson, C.F., Irwin, P.G.J., Belyaev, D.A., Patrakeev, A., Shakun, A., 2021. Seasonal
237 reappearance of HCl in the atmosphere of Mars year 35 dusty season. *A&A*. 647, A161.
238 <https://dx.doi.org/10.1051/0004-6361/202140329>.
- 239 Stern, J.C., Sutter, B., Freissinet, C., Navarro-González, R., McKay, C.P., Archer Jr., P.D.,
240 Buch, A., Brunner, A.E., Coll, P., Eigenbrode, J.L., Fairén, A.G., Franz, H.B., Glavin, D.P.,
241 Kashyap, S., McAdam, A.C., Ming, D.W., Steele, A., Szopa, C., Wray, J.J., Martín-Torres,
242 F.J., Zorzano, M.-P., Conrad, P.G., Mahaffy, P.R. and the MSL Science Team, 2015.
243 Evidence for indigenous nitrogen in sedimentary and aeolian deposits from the Curiosity
244 rover investigations at Gale crater, Mars. *PNAS*. 112, pp. 4245-4250.
245 <https://doi.org/10.1073/pnas.1420932112>.
- 246 Sutter, B., McAdam, A.C., Mahaffy, P.R., Ming, D.W., Edgett, K.S., Rampe, E.B., Eigenbrode,
247 J.L., Franz, H.B., Freissinet, C., Grotzinger, J.P., Steele, A., House, C.H., Archer, P.D.,
248 Malespin, C.A., Navarro-González, R., Stern, J.C., Bell, J.F., Calef, F.J., Gellert, R.,
249 Glavin, D.P., Thompson, L.M., Yen, A.S., 2017. Evolved gas analyses of sedimentary
250 rocks and eolian sediment in Gale Crater, Mars: Results of the Curiosity rover's sample
251 analysis at Mars instrument from Yellowknife Bay to the Namib Dune. *J. Geophys. Res.*
252 Planets. 122, pp. 2574-2609. <https://doi.org/10.1002/2016JE005225>.
- 253 Thelen, A.E., Nixon, C.A., Chanover, N.J., Cordiner, M.A., Molter, E.M., Teanby, N.A., Irwin,
254 P.G.J., Serigano, J., Charnley, S.B., 2019. Abundance measurements of Titan's
255 stratospheric HCN, HC3N, C3H4, and CH3CN from ALMA observations. *Icarus*. 319, pp.
256 417-432. <https://doi.org/10.1016/j.icarus.2018.09.023>.
- 257 Trokhimovskiy, A., Perevalov, V., Koralev, O., Fedorova, A.A., Olsen, K.S., Bertaux, J.-L.,
258 Patrakeev, A., Shakun, A., Montmessin, F., Lefèvre, F., Lukashevskaya, A., 2020. First
259 observation of the magnetic dipole CO₂ main isotopologue absorption band at 3.3 μm in
260 the atmosphere of Mars by ExoMars Trace Gas Orbiter ACS instrument. *A&A*. 639,
261 A142. <https://dx.doi.org/10.1051/0004-6361/202038134>.
- 262 Trokhimovskiy, A., Fedorova, A.A., Olsen, K.S., Alday, J., Koralev, O., Montmessin, F.,
263 Lefèvre, F., Patrakeev, A., Belyaev, D., Shakun, A.V., 2021. Isotopes of chlorine from HCl
264 in the Martian atmosphere. *A& A*. 651, A32. <https://doi.org/10.1051/0004-6361/202140916>.
- 266 Vago, J., Witasse, O., Svedhem, H., Baglioni, P., Haldemann, A., Gianfiglio, G., Blancquaert,
267 T., McCoy, D., de Groot, R., 2015. ESA ExoMars program: The next step in exploring
268 Mars. *Sol. Sys. Res.* 49, pp. 518-528. <https://doi.org/10.1134/S0038094615070199>.
- 269 Villanueva, G.L., Mumma, M.J., Novak, R.E., Radeva, Y.L., Käufl, H.U., Smette, A., Tokunaga,
270 A., Khayat, A., Encrenaz, T., Hartogh, P., 2013. A sensitive search for organics (CH₄,
271 CH₃OH, H₂CO, C₂H₆, C₂H₂, C₂H₄), hydroperoxy (HO₂), nitrogen compounds (N₂O,
272 NH₃, HCN) and chlorine species (HCl, CH₃Cl) on Mars using ground-based high-
273 resolution infrared spectroscopy. *Icarus*. 223, pp. 11-27.
274 <https://doi.org/10.1016/j.icarus.2012.11.013>.

275

276

277

278

279